

Amide–Iminol Tautomerism: Effect of Metalation

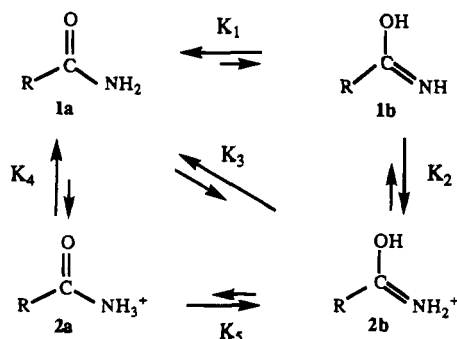
David P. Fairlie,^{*,†} Tai Chin Woon,[†]
Wasantha A. Wickramasinghe,[†] and
Anthony C. Willis[‡]

The 3D Centre, University of Queensland, Brisbane,
Qld 4072, Australia, and The Research School of Chemistry,
The Australian National University, Canberra,
ACT 2600, Australia

Received May 27, 1994

Introduction

Minor, often undetectable, tautomeric structures are frequently implicated as putative reaction intermediates in solution so it is important to find ways of stabilizing them to permit examination of their properties. In the case of carboxylic acid amides, the amide (**1a**) rather than iminol (**1b**) tautomeric structure is



adopted almost exclusively ($K_{1(\text{est})} \sim 10^8$)^{1b} and this is independent of the nature of R (e.g. H, alkyl, aryl, NH_2).¹ In strongly acidic solutions ($\text{pH} < 1$) the amide **1a** protonates preferentially² on the more basic oxygen atom (**2b**, $K_3 \sim 10^1$),^{1b} although a trace amount ($K_5 \geq 10^3$;³ $K_{5(\text{est})} \sim 10^7$;^{1b}) of N-protonation (**2a**) is believed^{1a} to account for some reactions of amides ($K_2 \sim 10^7$; $K_4 \sim 10^8$).^{1b}

On the other hand metalation of amides could occur at either oxygen or nitrogen. We now report that dienPt(II) can metalate amides at nitrogen and oxygen, but only N-coordination stabilizes both amide (NH_2COR) and iminol ($\text{NH}=\text{C}(\text{OH})\text{R}$) tautomers. Structures and properties of $[\text{dienPtNH}_2\text{COR}]^{2+}$ and $[\text{dienPtNH}=\text{C}(\text{OH})\text{R}]^{2+}$ are compared, the reported iminol structure $[(\text{NH}_3)_5\text{RhNH}=\text{C}(\text{OH})\text{R}]^{3+}$ ($\text{R} = \text{NH}_2$) is reinvestigated and found to be the alternative amide tautomeric form $[(\text{NH}_3)_5\text{RhNH}_2\text{COR}]^{3+}$, and rearrangements between the structures are discussed.

* Author to whom correspondence should be addressed.

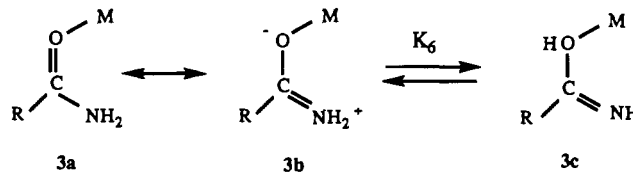
[†] University of Queensland.

[‡] The Australian National University.

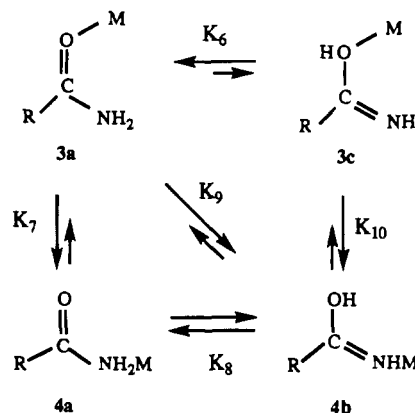
- (a) Zabicky, J., Ed. *The Chemistry of Amides*; J. Wiley-Interscience: New York, 1970; Chapter 1, p 1. (b) Sigel, H.; Martin, R. B. *Chem. Rev.* **1982**, *82*, 385.
- (a) Olah, G. A.; White, A. M. *J. Am. Chem. Soc.* **1968**, *90*, 6087. (b) Worshaw, J. E., Jr; Busing, W. R. *Acta Crystallogr., Sect. B*, **1969**, *B25*, 572. (c) Bryden, J. H. *Acta Crystallogr.* **1957**, *10*, 714. (d) Redpath, C. R.; Smith, J. A. S. *Trans. Faraday Soc.* **1962**, *58*, 462. (e) Arnett, E. M.; Mitchell, E. J.; Murty, T. S. S. R. *J. Am. Chem. Soc.* **1974**, *96*, 3875.
- Benderly, H.; Rosenheck, K. *J. Chem. Soc., Chem. Commun.* **1972**, 179.

Results and Discussion

When $[\text{dienPtOH}_2](\text{CF}_3\text{SO}_3)_2$ reacts in acetone with either acetamide or 1,1-dimethylurea, we were surprised^{1b,4} to find that there was exclusive metalation of the oxygen atom of **1a** to form $[\text{dienPtOCRNH}_2]^{2+}$ ($\text{R} = \text{Me}$ or NMe_2).⁵ The tautomeric form is unquestionably amide **3a**, including a contribution from canonical form **3b**, with no detectable iminol tautomer **3c**.⁶ However **3a** (analogous to **2b**) is unstable and the metal



migrates (linkage isomerization) in a few hours at 20 °C in acetone to the thermodynamically preferred nitrogen atom.⁵ Which tautomeric form of the stable N-metalated product is adopted, **4a** or **4b** (analogous to **2a** or **2b** respectively)?



The solid state structure for **4** ($\text{R} = \text{NMe}_2$) is established here by X-ray crystallography (Tables 1–3 and supplementary Tables 4–9) as **4a**, $[\text{dienPtNH}_2\text{CONMe}_2]^{2+}$, which is depicted in the ORTEP drawing (Figure 1). Although one of the triflate counter ions is somewhat disordered and affected the refinement, the observed amide bond lengths and angles (Table 3) nevertheless conclusively establish the structure as the rare^{1b} tautomer **4a**, rather than **4b**. For comparison of bond lengths and angles we also determined the X-ray structure⁷ of $\text{NH}_2\text{-CONMe}_2$ (Supplementary Tables 10–17).

The PtN_4 coordination geometry has the expected planarity with a mean Pt–N distance of 2.02 (2) Å. The dihedral angle between this plane and the planar dimethylurea ligand is 84.8°.

- (4) Amides are often N-bonded and/or bridged ligands for Pt: (a) Hollis, L. S.; Lippard, S. J. *J. Am. Chem. Soc.* **1981**, *103*, 6761. (b) Rochon, F. D.; Kong, P. C.; Melanson, R. *Inorg. Chem.* **1990**, *29*, 1352. (c) Cini, R.; Fanizzi, F. P.; Intini, F. P.; Maresca, L.; Natile, G. *J. Am. Chem. Soc.* **1993**, *115*, 5123.
- (a) Woon, T. C.; Fairlie, D. P. *Inorg. Chem.* **1992**, *31*, 4069. (b) Woon, T. C.; Wickramasinghe, W. A.; Fairlie, D. P. *Inorg. Chem.* **1993**, *32*, 2190.
- (6) The ¹³C-NMR spectra are diagnostic for O- versus N-coordination.⁵ **3a** was distinguished over **3c** in the ¹H NMR spectrum by the lack of a (OH) proton which should^{9,10} exchange with added acid/water. The contribution of canonical form **3b** in $[\text{dienPtOCMeNH}_2](\text{CF}_3\text{SO}_3)_2$ was revealed by the inequivalence in acetone-*d*₆ at 20 °C of the two amide NH protons ($\text{R} = \text{Me}$, 8.93, 8.49 ppm (amide NH, 2H) versus TMS) resulting from restricted rotation about the partial C=N amide bond.
- (7) X-ray structural data for $\text{NH}_2\text{CONMe}_2$: $\text{C}_3\text{H}_8\text{N}_2\text{O}$, fw = 88.1, $T = 163$ K, monoclinic, $P2_1/n$, $a = 8.572(3)$ Å, $b = 6.020(1)$ Å, $c = 9.270(3)$ Å, $\alpha = \gamma = 90^\circ$, $\beta = 108.70(3)^\circ$, $V = 453.1(3)$ Å³, $Z = 4$; R (R_w) = 0.035(0.038).

Table 1. Crystallographic Data for $[\text{Pt}(\text{C}_4\text{H}_{13}\text{N}_3)(\text{C}_3\text{H}_8\text{N}_2\text{O})](\text{CF}_3\text{SO}_3)_2$

formula	$\text{C}_9\text{H}_{21}\text{F}_6\text{N}_5\text{O}_7\text{PtS}_2$	cryst dimens, mm	$0.06 \times 0.08 \times 0.16$
fw	684.5	X-radiation	Cu K α
cryst syst	orthorhombic	λ , Å	1.5418
space group	<i>Pbca</i>	data range, ° in 2θ	4–120
<i>a</i> , Å	21.639(3)	no. of unique data	3201
<i>b</i> , Å	8.547(2)	no. of data refined	1778 [$I > 3\sigma(I)$]
<i>c</i> , Å	23.376(2)	no. of restraints	14
<i>V</i> , Å ³	4323.4(7)	no. of variables	271
<i>Z</i>	8	R^a	0.050
d_{calcd} , g cm ⁻³	2.103	R_w^b	0.068
μ [Mo K α], cm ⁻¹	148.3	GOF ^c	1.65
<i>T</i> , °C	20(1)	<i>F</i> (000)	2639.3

^a $R = \sum ||F_o| - |F_c|| / \sum |F_o|$. ^b $R_w = [\sum w(|F_o| - |F_c|)^2 / \sum (wF_o^2)]^{1/2}$.
^c GOF = $[\sum w(|F_c| - |F_o|)^2 / (\text{no. of ref} - \text{no. of var})]^{1/2}$.

Table 2. Atomic Coordinates and Isotropic Displacement Parameters for the Non-Hydrogen Atoms in $[\text{Pt}(\text{C}_4\text{H}_{13}\text{N}_3)(\text{C}_3\text{H}_8\text{N}_2\text{O})](\text{CF}_3\text{SO}_3)_2$

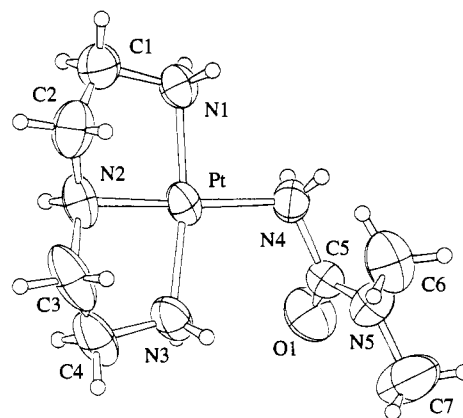
	<i>x/a</i>	<i>y/b</i>	<i>z/c</i>	U_{eq}^a , Å ²
Pt	0.45970(4)	0.45122(7)	0.59249(2)	0.0790(3)
O(1)	0.6144(8)	0.534(2)	0.5475(7)	0.135(7)
N(1)	0.3816(7)	0.570(1)	0.5721(6)	0.086(5)
N(2)	0.4012(9)	0.282(2)	0.6157(6)	0.100(6)
N(3)	0.5244(8)	0.306(2)	0.6222(6)	0.107(7)
N(4)	0.5169(7)	0.632(2)	0.5684(7)	0.102(6)
N(5)	0.6031(7)	0.662(2)	0.6298(5)	0.093(6)
C(1)	0.327(1)	0.459(2)	0.5813(9)	0.109(9)
C(2)	0.341(1)	0.353(3)	0.6294(9)	0.12(1)
C(3)	0.433(2)	0.190(2)	0.6644(9)	0.15(1)
C(4)	0.496(2)	0.158(2)	0.6409(9)	0.13(1)
C(5)	0.5842(9)	0.604(2)	0.5791(7)	0.078(7)
C(6)	0.564(1)	0.744(3)	0.673(1)	0.15(1)
C(7)	0.668(1)	0.640(4)	0.643(1)	0.18(2)
S(1)	0.3954(3)	0.7461(5)	0.2270(2)	0.100(2)
C(10)	0.3146(5)	0.728(2)	0.2410(8)	0.19(2)
F(11)	0.2979(9)	0.581(3)	0.225(1)	0.28(1)
F(12)	0.304(1)	0.757(4)	0.2972(9)	0.31(2)
F(13)	0.2853(8)	0.825(2)	0.204(1)	0.27(1)
O(11)	0.4106(7)	0.905(1)	0.2391(6)	0.137(7)
O(12)	0.403(1)	0.710(2)	0.1679(4)	0.173(9)
O(13)	0.4222(6)	0.632(1)	0.2641(5)	0.111(5)
S(2)	0.3960(3)	0.9629(5)	0.4965(2)	0.104(2)
C(20)	0.3245(6)	0.940(2)	0.4601(9)	0.17(2)
F(21)	0.2861(8)	1.064(2)	0.464(1)	0.23(1)
F(22)	0.337(1)	0.918(4)	0.4036(9)	0.31(2)
F(23)	0.2908(8)	0.822(2)	0.483(1)	0.27(1)
O(21)	0.4227(6)	0.815(1)	0.4933(7)	0.136(7)
O(22)	0.373(2)	0.991(3)	0.5521(7)	0.32(2)
O(23)	0.4204(9)	1.103(2)	0.478(1)	0.25(1)

$$^a U_{\text{eq}} = \frac{1}{3} \sum_i \sum_j U_{ij} a_i^* a_j^* a_i a_j$$

Comparison of the two crystal structures shows that the dimethylurea molecule undergoes substantial electronic reorganization upon N-coordination to platinum. The N(4)–C(5) bond lengthens significantly (from 1.347(3) to 1.50(3) Å) while the C(5)–O(1) carbonyl bond shortens significantly (1.259(3) to 1.15(2) Å). These features together with the N(4)–C(5)–N(5) angle (113(2)°) and the Pt–N(4)–C(5) angle (115(1)°) are characteristic of the $\text{PtNH}_2\text{CONMe}_2$ unit. They reveal that the lone pair electrons of N(4) that were partly delocalized into the N(4)–C(5) bond of free dimethylurea have now become utilized in bonding to platinum resulting in a single bond N(4)–C(5) and a localization of π -electron density in the O(1)–C(5)–N(5) portion of the molecule. Although the C(5)–N(5) bond length is not detectably shorter in the complex (1.35(2) Å) versus free ligand (1.357(4) Å), the methyl substituents appear as a doublet in the ¹³C-NMR spectrum⁸ at 20 °C for the complex compared with a singlet for the free dimethylurea. The ¹H-NMR

Table 3. Selected Interatomic Distances (Å) and Angles (deg) for $[\text{Pt}(\text{C}_4\text{H}_{13}\text{N}_3)(\text{C}_3\text{H}_8\text{N}_2\text{O})](\text{CF}_3\text{SO}_3)_2$

Pt–N(1)	2.03(1)	Pt–N(2)	2.00(2)
Pt–N(3)	1.99(2)	Pt–N(4)	2.06(2)
O(1)–C(5)	1.15(2)	N(1)–C(1)	1.53(3)
N(2)–C(2)	1.46(3)	N(2)–C(3)	1.55(3)
N(3)–C(4)	1.48(3)	N(4)–C(5)	1.50(3)
N(5)–C(5)	1.35(2)	N(5)–C(6)	1.49(3)
N(5)–C(7)	1.45(3)	C(1)–C(2)	1.48(3)
C(3)–C(4)	1.48(4)		
N(1)–Pt–N(2)	84.2(6)	N(1)–Pt–N(3)	167.9(6)
N(1)–Pt–N(4)	93.5(6)	N(2)–Pt–N(3)	84.3(7)
N(2)–Pt–N(4)	177.6(6)	N(3)–Pt–N(4)	98.0(6)
Pt–N(1)–C(1)	108(1)	Pt–N(2)–C(2)	109(1)
Pt–N(2)–C(3)	106(1)	C(2)–N(2)–C(3)	116(2)
Pt–N(3)–C(4)	110(2)	Pt–N(4)–C(5)	115(1)
C(5)–N(5)–C(6)	126(2)	C(5)–N(5)–C(7)	116(2)
C(6)–N(5)–C(7)	118(2)	N(1)–C(1)–C(2)	109(2)
N(2)–C(2)–C(1)	106(2)	N(2)–C(3)–C(4)	103(2)
N(3)–C(4)–C(3)	110(2)	O(1)–C(5)–N(4)	122(2)
O(1)–C(5)–N(5)	126(2)	N(4)–C(5)–N(5)	113(2)

**Figure 1.** ORTEP drawing of the cation of $[\text{dienPtNH}_2\text{CONMe}_2](\text{CF}_3\text{SO}_3)_2$ with 30% probability ellipsoids giving atomic numbering.

spectrum⁸ only exhibited a broad singlet for the NMe_2 group. The better resolved splitting in the ¹³C-NMR spectrum is indicative of a higher energy barrier to rotation about the C(5)–N(5) bond for the N-metalated ligand as expected for a (slight) increase in bond order. The alternative tautomer **4b** requires substantial shortening of the N(4)–C(5) bond and lengthening of the C(5)–O(1) bond (1.15(2) Å here), opposite trends to those observed here.

This same tautomeric form **4a**, $[\text{dienPtNH}_2\text{COR}]^{2+}$, is maintained in solution in $\text{OC}(\text{CD}_3)_2$ for $\text{R} = \text{NMe}_2$ (see Figure 2A). A key feature in the ¹H-NMR spectrum is the appearance of resonance A (~7 ppm) which integrates for two protons and must be assigned to the NH_2 of the dimethylurea ligand. On the other hand tautomer **4b** $[\text{dienPtNH}=\text{C}(\text{OH})\text{R}]^{2+}$ requires two low frequency urea resonances (NH,OH), each integrating for one proton and the OH in particular should^{9,10} undergo rapid exchange with added acid/water. Neither of these features was observed.

In contrast, the N-bonded acetamide complex ($\text{R} = \text{Me}$) shows separate ¹H-NMR signals (Figure 2B) in $\text{OC}(\text{CD}_3)_2$ for 3 different amide protons (OH, ~12 ppm; NH, ~8.5 ppm; Me,

- (8) $[\text{dienPtNH}_2\text{CONMe}_2](\text{CF}_3\text{SO}_3)_2$. ¹³C-NMR data (δ , TMS) in acetone-*d*₆: 157.7 (C=O); 55.0, 51.4 (dien), 37.7, 37.1 (NMe₂). ¹H-NMR data (δ , TMS) in acetone-*d*₆: 7.07 (2H, ureaNH₂); 6.83 (1H, dienNH); 5.54, 5.29 (4H, dienNH₂); 2.8–3.4 (8H, dienCH₂), 3.00 (br, 6H, NMe₂). $[\text{dienPtNH}=\text{C}(\text{OH})\text{Me}](\text{CF}_3\text{SO}_3)_2$. ¹³C-NMR data (δ , TMS) in acetone-*d*₆: 177.4 (C=O); 54.7, 51.9 (dien), 21.4 (Me). ¹H-NMR data (δ , TMS) in acetone-*d*₆: 12.0 (1H, OH); 8.46 (1H, PtNH=C); 6.49 (1H, dienNH); 5.43, 5.52 (4H, dienNH₂); 2.5–3.5 (8H, dienCH₂), 2.27 (br, 3H, Me).

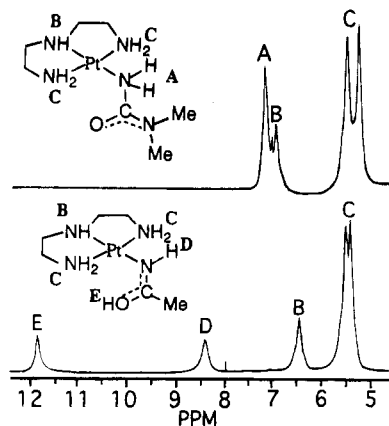


Figure 2. 300 MHz $^1\text{H-NMR}$ spectra (NH/OH region only) for dry acetone- d_6 solutions of $[\text{dienPtNH}_2\text{CONMe}_2](\text{CF}_3\text{SO}_3)_2$ (A, top) and $[\text{dienPtNH}=\text{C}(\text{OH})\text{Me}](\text{CF}_3\text{SO}_3)_2$ (B, bottom). Scale is δ relative to TMS.

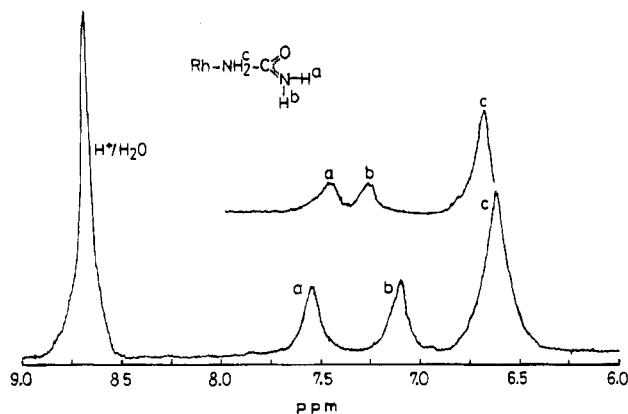


Figure 3. 100 MHz $^1\text{H-NMR}$ spectra (urea/water/ H^+ region only) for $[(\text{NH}_3)_5\text{RhNH}_2\text{CONH}_2](\text{NO}_3)_3$ in $\text{DMSO-}d_6$ with added $\text{H}^+/\text{H}_2\text{O}$ at 293 K and (inset) 313 K. Scale is δ relative to TMS.

~ 2 ppm),⁸ compared to the two (NH, Me) observed for the dimethylurea complex. The two lowest field resonances are characteristic of the increased anisotropy of the $\text{C}(\text{=NH})\text{OH}$ group. Also added water/acid exchanges with the group giving rise to signal E, which shifts downfield with H^+ and increases in intensity. These contrasting NMR spectra establish that the different tautomeric solution structure **4b**, $[\text{dienPtNH}=\text{C}(\text{OH})\text{R}]^{2+}$, was being observed for the N-metalated acetamide.

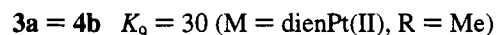
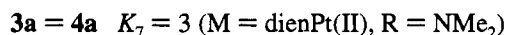
In view of these data, we also reinvestigated the solution structures of the known¹¹ $(\text{NH}_3)_5\text{Rh}^{\text{III}}$ complexes of urea ($\text{R} = \text{NH}_2$). Isolated complexes of both N- and O-bonded urea are unstable ($K_7 \sim 1$), but the isomerization $4 \rightarrow 3\text{a}$ is sufficiently slow¹¹ that the predominant tautomeric form for the nitrogen bonded linkage isomer of urea (**4a** or **4b**) could be deduced. A previous interpretation¹¹ of the $^1\text{H-NMR}$ spectrum for the N-bonded urea favored tautomer **4b**, $[(\text{NH}_3)_5\text{RhNH}=\text{C}(\text{OH})\text{-NH}_2]^{3+}$. This structure requires three (or four) separate ^1H signals for the urea ligand, three were observed (Figure 3) in the required ratio (2:1:1). However one of these, the acidic OH, should^{9,10} exchange with added H^+ or OH_2 . As shown in Figure 3, added H^+ does not alter the positions or intensities of

the three resonances (a, b, c) and no exchange was detected several hours later. Moreover, the two single proton resonances (a, b) were found to begin coalescing about an invariant midpoint as the temperature was raised (inset, Figure 3). These two important observations are consistent only with (greater) restricted rotation about the $\text{C}=\text{NH}_2$ bond expected for **4a** and firmly establishes the assignment of the tautomeric structure as $[(\text{NH}_3)_5\text{RhNH}_2\text{CONH}_2]^{3+}$, akin to that reported here for $[\text{dienPtNH}_2\text{CONMe}_2]^{2+}$.

These results reveal that the substituent R influences the thermodynamic preference for tautomers **4a** versus **4b** and the magnitude of K_8 . On the basis of only one tautomer being detected by NMR spectroscopy in each case, K_8 is estimated at $\geq 10^2$ for $\text{R} = \text{Me}$ but $\leq 10^2$ for $\text{R} = \text{NMe}_2$. This difference results from more dispersed π -electron density in the urea versus acetamide making the oxygen less basic than nitrogen in the urea complex. This contrasts starkly with free acetamide and free urea, where oxygen is more basic and is selectively protonated in each case. Thus the metal is crucial for stabilizing the observed tautomers.

Based on these results for Pt(II) and Rh(III), we can now interpret previous experiments with "amides" bonded either to $(\text{NH}_3)_5\text{Ru}(\text{III})$, where the metal was paramagnetic so that tautomers could not be unequivocally deduced,¹² or to $(\text{NH}_3)_5\text{-Co}(\text{III})$ and $(\text{NH}_3)_5\text{Ru}(\text{II})$ and $(\text{NH}_3)_5\text{Cr}(\text{III})$, where the metal rapidly migrated from nitrogen to oxygen of the uncharged "amide" ligand both in solution and the solid state ($K_8 \leq 10^{-2}$).^{10,12b,13} We now infer that the iminol tautomer **4b** likely prevailed for acetamide ($\text{R} = \text{Me}$) while the amide tautomer **4a** was likely preferred for ureas ($\text{R} = \text{NH}_2, \text{NMe}_2$) in these cases as well.

It has been suggested^{5,10,12} that rearrangements between **3a** and **4b** may be mediated by **4a**. For amides where $\text{R} = \text{H}$, alkyl or aryl, **4a** has still never been detected in metal complexes. The suggestion derives from the difference in rates of metal migration from **3** to **4** and **4** to **3**, these being slower for $\text{R} = \text{Me}$ than $\text{R} = \text{NMe}_2$. For $\text{R} = \text{NMe}_2$, this rearrangement likely proceeds directly between **3** and **4a**. For $\text{R} = \text{Me}$, significant π -electronic reorganizations would have to take place in the amide ligand to accommodate successive interconversions $3\text{a} \leftrightarrow 4\text{a} \leftrightarrow 4\text{b}$. Using the observed⁵ equilibrium constants:



an estimate for $\text{R} = \text{Me}$ of $K_8 = [4\text{b}/4\text{a}]$ in acetone is the ratio $K_9/K_7 = 10$, assuming that K_7 is similar for $\text{R} = \text{Me}$ and $\text{R} = \text{NMe}_2$. This is likely to be an underestimate because **4a** ($\text{R} = \text{Me}$) is expected to be less stable than **4a** ($\text{R} = \text{NMe}_2$) and hence the equilibrium constant K_8 should be larger, possibly $\geq 10^3$ as estimated³ for the respective tautomers of protonated free amides **2a** and **2b**. Alternatively, using the measured acidities in water of $[\text{dienPtNH}_2\text{CONMe}_2]^{2+}$ versus $[\text{dienPtNH}=\text{C}(\text{OH})\text{Me}]^{2+}$ (5.6 vs 3.8, 20 °C, $I = 0.025 \text{ M}$ vs 0.1 M),⁵ and by assuming the conjugate bases $[\text{dienPtNHCOR}]^+$ ($\text{R} = \text{Me}, \text{NMe}_2$) have similar amide electronic structures,¹⁴ the two $\text{p}K_a$ units difference in acidities suggests $K_8 \sim 10^2$.



(9) Buckingham, D. A.; Keene, R. F.; Sargeson, A. M. *J. Am. Chem. Soc.* **1973**, *95*, 5649.

(10) Co^{III} -amides and Co^{III} -ureas: (a) Angel, R. L.; Fairlie, D. P.; Jackson, W. G. *Inorg. Chem.* **1990**, *29*, 20. (b) Dixon, N. E.; Fairlie, D. P.; Jackson, W. G.; Sargeson, A. M. *Inorg. Chem.* **1983**, *22*, 4083. (c) Fairlie, D. P.; Jackson, W. G. *Inorg. Chim. Acta*, **1988**, *150*, 81.

(11) Rh^{III} -ureas: Curtis, N. J.; Dixon, N. E.; Sargeson, A. M. *J. Am. Chem. Soc.* **1983**, *105*, 5347.

(12) Ru^{III} -ureas and Ru^{III} -amides: (a) Fairlie, D. P.; Taube, H. *Inorg. Chem.* **1985**, *24*, 3199. (b) Fairlie, D. P.; Ilan, Y.; Taube, H. *Inorg. Chem.*, submitted for publication.

(13) Cr^{III} -amides: Curtis, N. J.; Lawrance, G. A.; Sargeson, A. M. *Aust. J. Chem.* **1983**, *36*, 1495.

Finally, the differences in linkage isomerization rates ($k_{34} = 6.4 \times 10^{-4} \text{ s}^{-1}$, R = NMe₂ vs $6.8 \times 10^{-6} \text{ s}^{-1}$, R = Me; and $k_{43} = \sim 2 \times 10^{-4} \text{ s}^{-1}$, R = NMe₂ vs $\sim 2.3 \times 10^{-7} \text{ s}^{-1}$, R = Me), measured or extracted from equilibrium and rate constants,⁵ are also consistent with $K_3 \sim 10^2\text{--}10^3$. We can therefore conclude from these equilibrium constants that the energy differences between tautomeric forms **3a**, **4a**, **4b** are relatively small ($\Delta G^0 = RT \ln K \sim 10\text{--}15 \text{ kJ mol}^{-1}$) indicating that the stabilizing effect of the metal need not be large to allow observation of the different amide tautomers and linkage isomers.^{5,10-14}

Experimental Section

NMR spectra (¹H, ¹³C) were recorded for all compounds on a Varian Gemini 300 MHz NMR spectrometer for acetone-*d*₆ or DMSO-*d*₆ solutions (at 293 K unless otherwise stated) containing tetramethylsilane as internal standard. The platinum compounds were synthesized from [dienPt(OH)₂](CF₃SO₃)₂ as reported elsewhere: [dienPtOC(NH₂)Me](CF₃SO₃)₂,^{5a} [dienPtOC(NH₂)NMe₂](CF₃SO₃)₂,^{5b} [dienPt NH₂CONMe₂](CF₃SO₃)₂,^{5b} [dienPtNH=C(OH)Me](CF₃SO₃)₂,^{5a} [dienPtNH-COMe](CF₃SO₃)₂,^{5a} [dienPtNHCONMe₂](CF₃SO₃)₂,^{5b} [(NH₃)₅RhNH=C(OH)NH₂]³⁺ was synthesized as described,¹¹ purified as the conjugate base by cation exchange chromatography on SP-C25 sephadex resin using aqueous Tris buffer (0.1 M, pH 8.5) containing NaNO₃ (0.1–0.5 M). The product was protonated in 0.1 M HNO₃ and isolated solid or generated directly in DMSO-*d*₆ solution by addition of CF₃SO₃H.

X-ray Data Collection and Structure Refinement. Crystals of [Pt(C₄H₁₃N₃)(C₃H₈N₂O)](CF₃SO₃)₂ were obtained from an acetone-diethyl ether solution. A colorless crystal was mounted on a Rigaku AFC6R diffractometer equipped with a graphite monochromator and attached to a Rigaku RU-200B rotating anode X-ray generator with a copper target. Twenty reflections were located and indexed on a primitive orthorhombic cell and Laue *mmm* symmetry was confirmed. Accurate lattice parameters were determined by least-squares analysis of the setting angles of 25 reflections $81 < 2\theta < 93^\circ$ using $\lambda(\text{Cu K}\alpha_1) = 1.54060 \text{ \AA}$. Crystallographic data are given in Table 1. Intensity data for reflections *h, k, -l* (*h*: 0 → 24, *k*: 0 → 9, *l*: -26 → 0) were

collected using $\omega\text{--}2\theta$ scans of width $(1.4 + 0.346 \tan \theta)^\circ$ in ω at a rate of 8° min^{-1} in ω , weak reflections being rescanned up to three times more to ensure good counting statistics. Background counts were taken for one quarter of the scan time on each side of every scan. Three standards measured at intervals of 150 min showed a 15% decrease in their intensities during data collection; data were corrected accordingly. Data were also corrected for absorption (transmission range 0.312–0.473).

The structure was solved by Patterson and difference-Fourier techniques. Anisotropic displacement factors were used for all non-hydrogen atoms. Hydrogen atoms were placed at calculated positions and included in the structure factor calculations but their parameters were not refined. Waser restraints¹⁵ were required to yield sensible bond lengths within the triflate groups. In addition, anisotropic displacement factors for some of the triflate atoms refine to very large values, probably indicating disorder which could not be simply modeled otherwise. Refinement was continued until all shift/error ratios were < 0.05.

Least-squares refinement was performed using full-matrix methods minimising the function $\sum w(|F_o| - |F_c|)^2$ where $w = [\sigma^2(F) + (0.0009)F^2]^{-1}$. Maximum and minimum heights in a final difference map were 0.84(5) and 0.99(5) e Å⁻³, respectively. Data reduction and refinement computations were performed with XTAL3.2;¹⁶ atomic scattering factors for neutral atoms and real and imaginary dispersion terms were taken from ref 17.

Supplementary Material Available: Supplementary Tables 4–9 (for [dienPtNH₂CONMe₂](CF₃SO₃)₂) and Tables 10–17 (for NH₂CONMe₂), giving atomic coordinates and isotropic displacement parameters for non-hydrogen and hydrogen atoms, anisotropic thermal parameters, bond distances and angles not included above, and selected least-squares planes, a table of crystal and data collection parameters for NH₂CONMe₂, and an ORTEP drawing for NH₂CONMe₂ (22 pages). Ordering information is given on any current masthead page. Listings of observed and calculated structure factors (12 pages) are available directly from the authors upon request.

(14) The X-ray crystal structures for the corresponding conjugate bases, [(NH₃)₅CoNHCOR]²⁺ (R = Me versus NHPH), gave amide bond lengths that were almost indistinguishable. (a) Schneider, M. L.; Ferguson, G.; Balahura, R. J. *Can. J. Chem.* **1973**, *51*, 2180. (b) Fairlie, D. P.; Jackson, W. G.; McLaughlin, G. M. *Inorg. Chem.* **1989**, *28*, 1983.

(15) Waser, J. *Acta Crystallogr.* **1963**, *16*, 1091–1094. Olthof-Hazekamp, R. CRYLSQ in ref 16. Restraints applied: S–C, 1.79(1) Å; S–O, 1.41(1) Å; C–F, 1.37(1) Å.

(16) Hall, S. R.; Flack, H. D.; Stewart, J. M., Eds. *XTAL3.2 Reference Manual*; Lamb: Perth, 1992.

(17) *International Tables for X-ray Crystallography*; Kynoch Press: Birmingham, England, 1974; Vol. IV, pp 99–101, 149–150 (distributed by Kluwer Academic Publishers, Dordrecht, The Netherlands).